ELSEVIER

PII: S0267-7261(97)00015-8

Soil Dynamics and Earthquake Engineering **16** (1997) 459–470

0267-7261/97/$17.00

Soil–structure interaction analysis of the Hualien containment model

Todor Ganev[a], Fumio Yamazaki[a], Tsuneo Katayama[b] & Teruyuki Ueshima[c]

[a]*Institute of Industrial Science, The University of Tokyo, 7-22-1 Roppongi, Minato-ku, Tokyo 106, Japan*
[b]*National Research Institute For Earth Science and Disaster Prevention, Tennodai, Tsukuba 305, Japan*
[c]*Central Research Institute of Electric Power Industry, 1646 Abiko, Abiko 270-11, Japan*

(Received 1 December 1996; revised 7 May 1997; accepted 7 May 1997)

This paper presents results from forced vibration tests, microtremor observations and earthquake response analysis of a nuclear reactor containment model constructed on stiff soil in Hualien, Taiwan. The dynamic behavior of the soil–structure system is simulated successfully with two numerical models: a sway-rocking model, whose soil parameters are evaluated on the basis of the continuum formulation method, and a finite element model, using the program SASSI with the flexible volume substructuring approach. The dependences of the soil parameters of both models on the amplitudes of the different dynamic excitations are investigated in detail. An original numerical simulation of microtremor is performed. Comparison with results of a previous study involving a rigid tower on a soft soil site in Chiba, Japan is offered.
© 1997 Elsevier Science Limited.

Keywords: soil–structure interaction, microtremor, forced vibration test, continuum formulation method, finite element method.

1 INTRODUCTION

The Hualien Large-Scale Seismic Test is an international project on dynamic soil–structure interaction. It is sponsored by a consortium of industrial and research enterprises from five countries (Japan, USA, Taiwan, France and Korea). The Hualien project has been initiated as a continuation of the Lotung Large-Scale Seismic Experiment [1]. Both test programs have involved construction of nuclear power plant containment models and monitoring of their earthquake response in conjunction with the surrounding soil. The Lotung Experiment has been carried out on soft soil. It has provided valuable data and insight into the complex interaction phenomena. In its turn, the Hualien Model has been constructed on stiff soil following the need to confirm and expand the findings of the previous program [2]. Hualien is located south of Lotung on the east coast of Taiwan, in a highly active seismic zone near the Philippine Sea Plate boundary.

It is of practical interest to compare the interaction effects, which occur at stiff and soft soil sites, and to seek integrated quantitative interpretations for analysis and design purposes. Following such an objective, this paper presents results from forced vibration tests, microtremor observations and earthquake response analysis of the Hualien Model. Soil–structure effects are identified from the recorded data. Considering these phenomena, the dynamic behavior of the soil–structure system is simulated with two numerical models. As the problem is non-trivial and complicated in many aspects, the obtained results could have useful implications to analysis and design practice. The case study of numerical analysis of microtremor, which is included in this paper, is a step towards a methodology for accurate computation of system functions on the basis of microtremor data.

The present authors have previously investigated the soil–struucture interaction of a reinforced concrete tower, constructed on soft soil in Chiba, Japan [3]. A comparison between the results of the two studies is offered.

2 DESCRIPTION OF THE MODEL AND THE EXPERIMENTAL DATA

The test structure (Fig. 1) represents a one-fourth scale model of a nuclear power plant containment. Its dimensions

Fig. 1. View of the containment model.

are shown in Fig. 2. The depth of the embedment is 5 m, which is 31% of the total height. The weight of the whole structure is 14 128 kN (1440.2 tf). 46% of the total mass is concentrated in the foundation and 35% in the roof.

Accelerometers are installed at all points of interest on the structure, as illustrated in Fig. 3. Surface and downhole seismometers, monitoring the motion of the soil are arranged in a three-dimensional array around the structure. Their locations are shown in Fig. 4.

The properties of the soil around and beneath the structure have been systematically investigated by in situ tests which comprise borings, large penetration tests and PS-loggings and laboratory tests which include triaxial tests on frozen undisturbed samples [4]. Based on the geotechnical investigation, the Central Research Institute of Electric Power Industry (CRIEPI), Japan, created a soil model of the foundation ground. This model was named the 'unified ground model' [5] and was used by all the participants in the Hualien Project. Subsequently, some of the soil properties were revised, following geotechnical investigations performed by CRIEPI in October 1994, and a 'modified ground model' was suggested. The unified model and its modification are presented in Fig. 5.

Two forced vibration tests (FVT) have been conducted on the Hualien Model: in October 1992 before backfill (FVT-1) and in February 1993 after backfill (FVT-2). In October 1994, the present authors conducted a series of microtremor observations of the structure and the surrounding soil using eight velocity-type pick-ups simultaneously.

Ganev et al. [6] determined the orientation errors of the free field accelerometers on the basis of earthquake data by

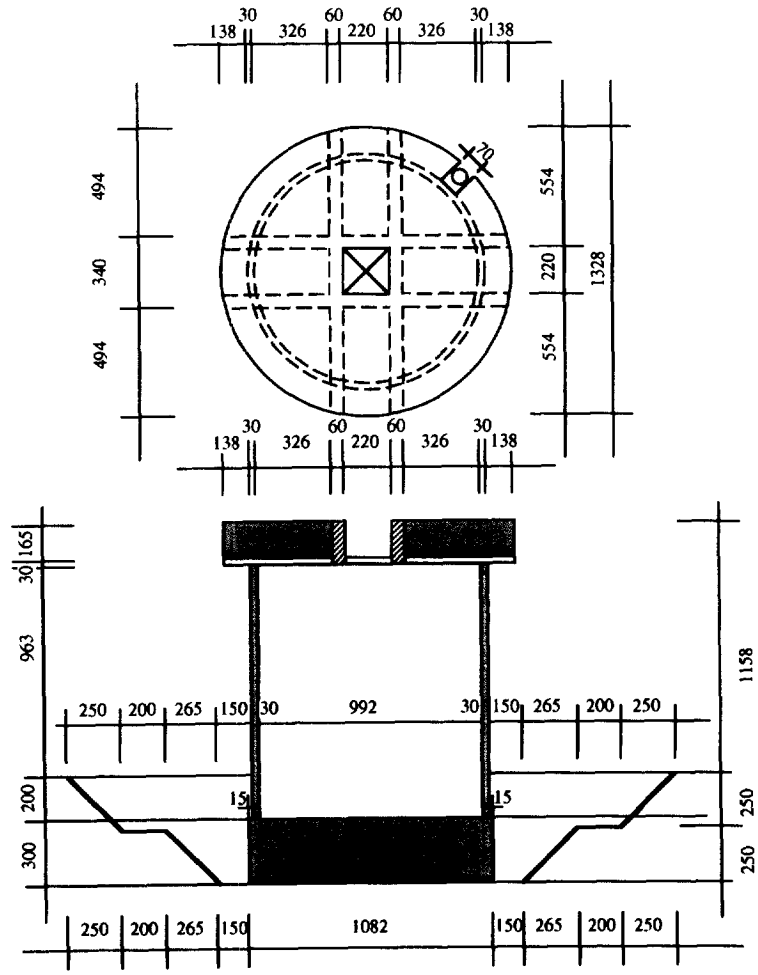

Fig. 2. Plan and vertical cross-section of the containment model (dimensions in cm).

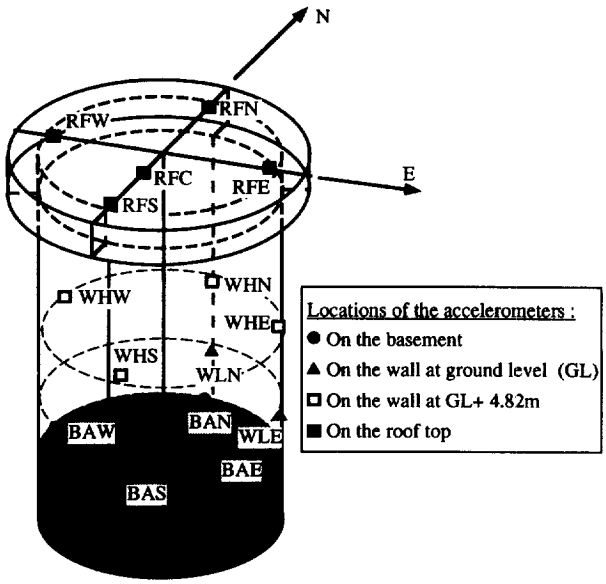

Fig. 3. Locations of the accelerometers on the structure.

means of the maximum cross-correlation method [7]. It was established that the records of surface station A15 (Fig. 4), which had often been used as control motions for numerical analysis, need correction. Counterclockwise rotation by 13° is recommended.

Before the backfill was completed, the excavation was flooded by heavy rains and its slopes partially collapsed. This is believed to have created anisotropic conditions in the vicinity of the foundation, which cause cross-axis coupling of the horizontal response of the structure. To minimize this effect, analysis can be conducted in the directions of the principal axes, which have been designated D1 and D2 [8,9]. Their position is found through rotating the geographical coordinate system counterclockwise by 61°.

During the construction of the roof slab, twelve enormous holes were made in the upper part of the shell wall, in order to insert temporary supporting beams for the formwork. Upon completion, the reinforcing bars were reconnected and the holes were filled, but the overall stiffness of the wall was rendered significantly less than initially intended. For this reason, in the numerical models described below, the Young modulus of the concrete was determined by trial and error to be $2.0 \times 10^{10}\,\mathrm{N\,m^{-2}}$, lower than the initial estimate of $2.6 \times 10^{10}\,\mathrm{N\,m^{-2}}$, which is based on the 28-day cylinder strength. Previous researchers [10] have obtained a similar value from inversion of structural response during FVT-1.

Data from five earthquakes recorded at the Hualien site are used in this study. Basic information about the events is presented in Tables 1, 2 and 3.

3 IDENTIFICATION OF SYSTEM CHARACTERISTICS

Fig. 6 presents a formal comparison between the results of FVT-2 and analysis of microtremor. The Fourier spectrum

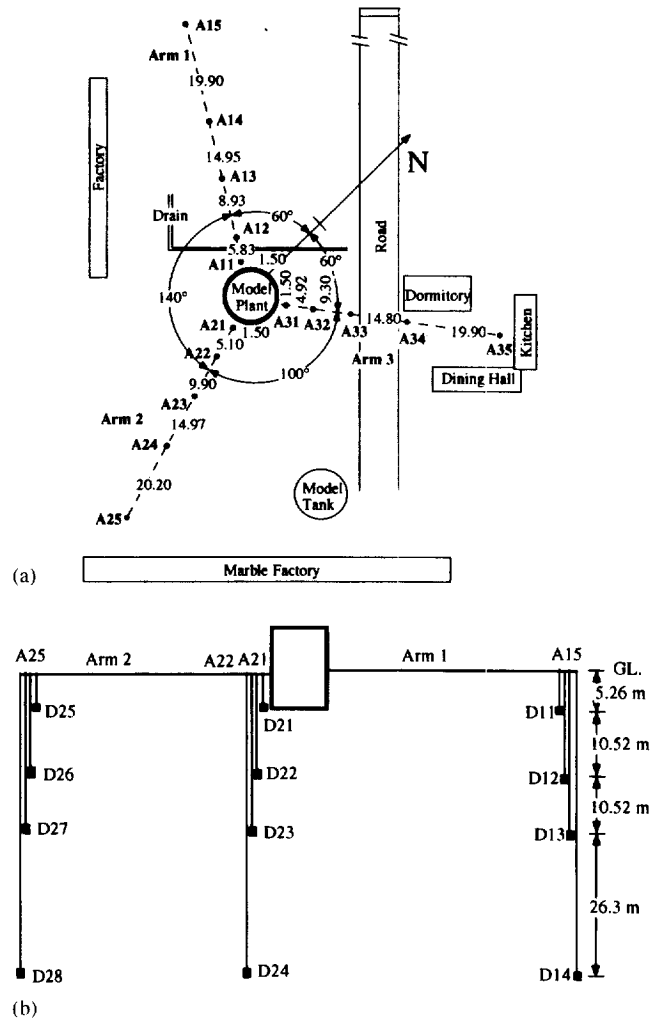

Fig. 4. Locations of the accelerometers at the experimental site: (a) plan of the site, (b) vertical cross-section of the site.

ratio between the roof response and the surrounding soil surface is evaluated from microtremor data and is plotted relative to the left side axis. The normalized amplitude of the roof response to base excitation is plotted for FVT-2 relative to the right side axis. The NS direction is used for this illustration, because the microtremor observations in the North–South and East–West directions were carried out at different times and rotation to the principal axes would not be completely accurate. The predominant frequency of the system is identified as 6.4 Hz from FVT and 6.3 Hz from

Table 1. Earthquake events used in the analysis

Event	Date	Epicenter		Magnitude
	mm/dd/yy	Latitude	Longitude	
940120	01/20/94	24°03′36″N	121°51′00″E	5.6
940530	05/30/94	24°05′40″N	121°34′20″E	4.5
940605	06/05/94	24°27′60″N	121°50′40″E	6.2
950501	05/01/95	24°02′42″N	121°39′06″E	4.9
950502	05/02/95	24°00′44″N	121°38′24″E	4.6

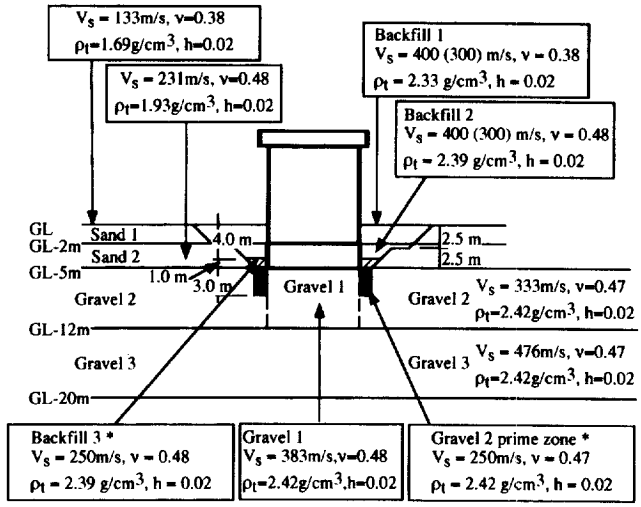

Notes:
Values in parentheses are those of the modified ground model.
Zones designated by asterisk (*) have been introduced in the modified ground model.

Fig. 5. The unified and modified ground models by CRIEPI.

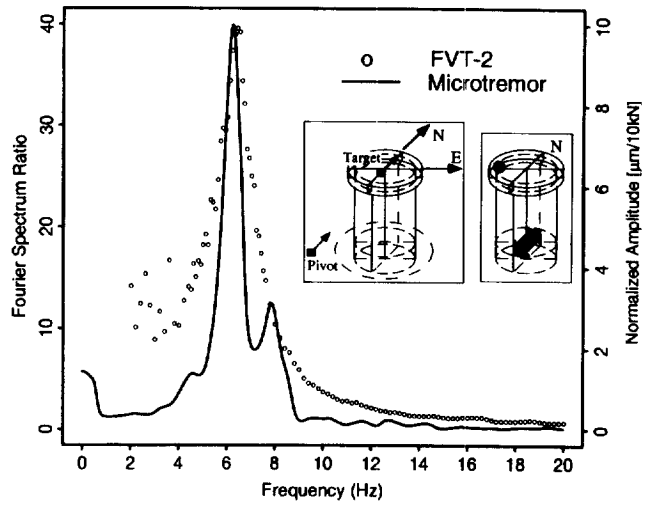

Fig. 6. Formal comparison between FVT-2 and microtremor.

microtremor. This good agreement shows that microtremor observation can be used successfully instead of forced vibration tests to evaluate system characteristics. Compared with the forced vibration tests, microtremor observation is easy and inexpensive to perform. Also, from a theoretical point of view, microtremor is closer to earthquake excitation than FVT, and permits a similar type of analysis. A shortcoming of microtremor observation is that owing to uncertainties in the nature of the vibrations, it is difficult to evaluate indubitably the soil–structure system amplification. This topic is discussed more in detail further on.

Fig. 7 shows Fourier spectrum ratios between the free field and the top of the structure, evaluated from earthquake records in the D2 direction. The predominant frequency of the system shifts from about 6.0 Hz for Event 940530 through 5.7 Hz for Event 940120 to 5.3 Hz for Event 950501. A similar decrease in predominant frequency as the ground motion becomes stronger, was observed previously by Ganev et al. [3] at a structure built on soft soil. The reason for the shift of the predominant frequency is weakening of the soil support during earthquakes. This phenomenon can usually be explained with three factors: soil non-linearity, separation of soil from the structure and pore water pressure build-up. At this point, no clear evidence of separation or pore water pressure build-up has been obtained, although relevant analysis has been performed. Most probably, the degradation of soil stiffness under dynamic loads is due to highly non-linear behavior as a result of local stress concentration at the contact with the foundation. This topic is discussed more in detail below in relation to the results of the simulation of the earthquake response with a finite element model.

4 NUMERICAL MODELING

Analysis of the structural response to FVT-2 was used as a starting point to establish suitable models for numerical simulation. The problem was approached in two different ways as described below.

4.1 Sway-rocking model

The behavior of the soil–structure system was simulated using the linear sway-rocking model shown in Fig. 8. The values of the soil springs and dashpots were determined on the basis of the continuum formulation method (CFM), developed by Harada et al. [11–14]. According to the provisions of the CFM, the sway spring K_H and dashpot C_H are to be evaluated for the whole embedment depth. In this case, however, while the stiffness of the massive fundament can be assumed infinite, it is recognized that

Table 2. Recorded peak acceleration (cm s^{-2}) at main points of interest

Event	D1			D2		
	Ground	Basement	Roof	Ground	Basement	Roof
940120	36.65	30.22	79.47	26.56	24.93	55.09
940530	32.16	11.43	28.90	19.54	12.32	33.59
940605	24.52	24.58	61.77	28.11	22.66	52.39
950501	66.42	55.83	84.63	99.76	72.76	165.24
950502	38.56	26.12	72.72	58.43	22.74	64.46

Table 3. Recorded peak velocity (cm s^{-1}) at main points of interest

Event	D1			D2		
	Ground	Basement	Roof	Ground	Basement	Roof
940120	2.07	2.38	3.39	1.68	1.50	2.24
940530	0.90	0.69	0.93	0.67	0.65	1.10
940605	3.74	4.44	4.35	3.05	3.26	3.75
950501	5.01	4.93	5.73	5.83	5.48	7.90
950502	2.05	1.83	2.51	1.61	1.23	2.42

the embedded part of the wall is deformable. This necessitates the division of the global K_H and C_H proportionally to the dimensions of each embedded part as illustrated in Fig. 8.

This analysis was initially performed using soil properties according to the unified ground model (Fig. 5). Subsequently, with the creation of the modified model (Fig. 5), the calculations were repeated with the revised parameters. The results of the two simulations are discussed further on in comparison with the finite element analysis.

4.2 Finite element model (SASSI)

Alternatively, dynamic analysis was performed with the program SASSI employing the flexible volume substructuring approach [15]. Taking advantage of the symmetry of the structure, a three-dimensional quarter model (Fig. 9) was used, and slightly different properties of the layer below the foundation were considered for the D1 and D2 directions. A more detailed scheme of the finite element discretization is shown in Fig. 10. By the time of this analysis, results of the latest geotechnical investigations performed by CRIEPI at the Hualien site were already available. Consequently, revised soil properties as prescribed by the modified ground model (Fig. 5) were used for the finite element model.

At the initial stage, the properties of material types 5 and 7 (Fig. 10(a)) were assumed equal to type 4. In this way, a softer ring of thickness 1.5 m is formed around the foundation. A plan of the discretization of the ring is shown in Fig. 10(b). The element numbering corresponds to the surface layer with thickness 1.0 m. This approximation is based on the assumption of the existence of a softer annular region around the foundation walls [16]. Previous analysis of the forced vibration test by Tang and Nakamura [17] has confirmed the feasibility of such an approach. The material properties used for simulation of the response in the D2 direction at the initial stage of the analysis can be seen in Table 4 in the column labeled FVT.

The records at surface station A14 (Fig. 4) were used as control motions for earthquake response analysis with both models.

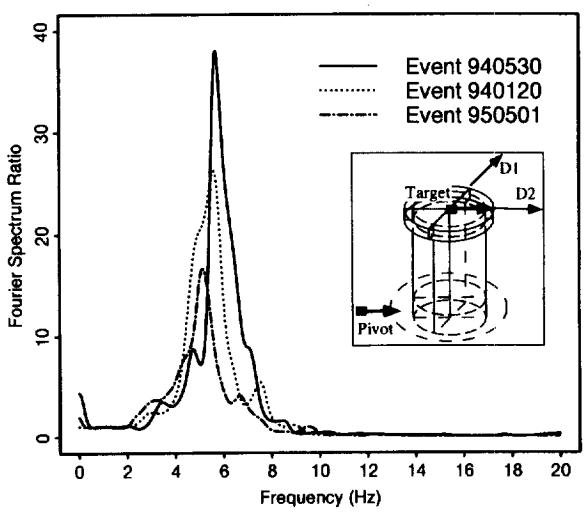

Fig. 7. Fourier spectrum ratios between the free field and the top of the structure.

5 DYNAMIC RESPONSE IN THE SMALL STRAIN RANGE

5.1 Forced vibration tests and a small earthquake

Initially, the results of FVT-2, which represent small-strain linear behavior, were simulated with both numerical models. Fig. 11 shows the recorded and calculated roof response to base excitation in the D2 direction. A very good agreement was produced by the analysis with SASSI, based on the modified ground model. However, in the case of the CFM simulation, better results were obtained using the soil properties of the unified model. This discrepancy provides some useful insight into the practice of numerical analysis. As can be seen in Fig. 5, the shear

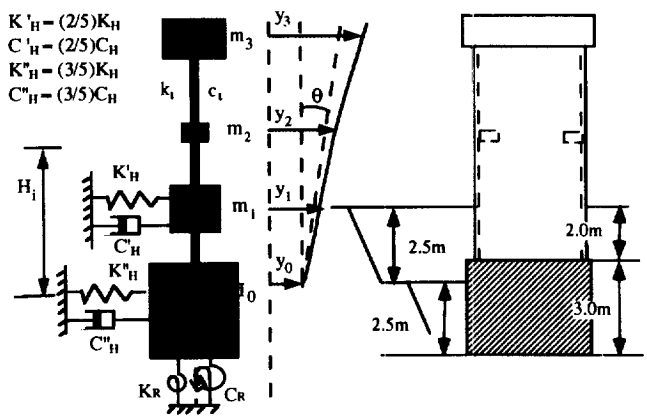

Fig. 8. Sway-rocking model.

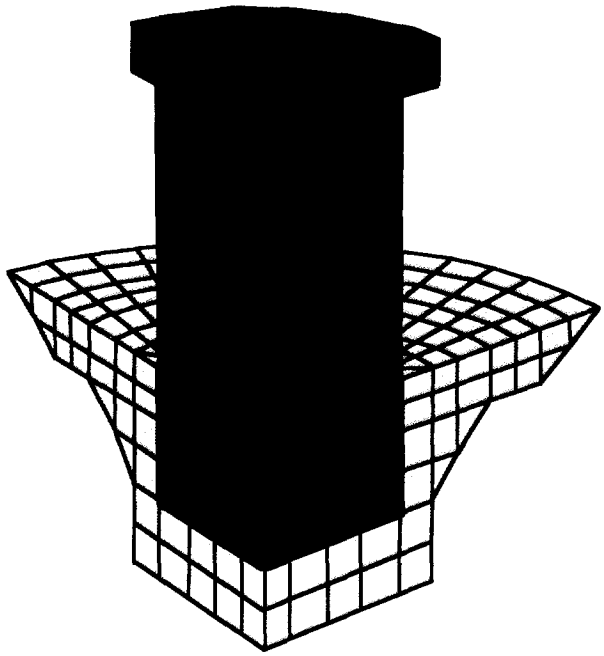

Fig. 9. Three-dimensional quarter model (SASSI).

wave velocity and respectively the stiffness of the backfills in the unified ground model are higher than those of the more reliable modified model and apparently exceed the actual values. The fact that the sway-rocking model utilized such a disparity to yield a good agreement, signifies that the CFM tends to underestimate the soil stiffness.

The reasons for this tendency are in the theoretical basis of the method. The soil reaction acting upon the side walls of the foundation is evaluated first for a unit thickness of the soil and then for the whole embedment depth [11,13]. This is equivalent to assuming a plane strain state along the vertical axis. Such an approach is accurate enough for evaluating the reaction to sway, because there is no relative displacement between different layers with unit thickness. However, in the case of rocking, different layers deform unevenly and the plane strain state assumption leads to neglect of some of the shear resistance of the soil. Such a tendency can surely be expected upon application of other similar and popular methods of analysis as, for example, the Novak model [18]. This conclusion has an important implication to design and might be of particular interest to practising engineers.

Following the successful simulation of FVT-2, both numerical models were validated by analyzing earthquake Event 940530, which had caused a very small relative structural response (c.f. Table 2) and no pronounced non-linear effects. The agreement with the actual response of the soil–structure system was very good in the D1 direction and with negligible discrepancy in the D2 direction. Using the unified ground model again yielded better results for the sway-rocking model.

While the SASSI analysis required detailed information about the site properties and elaborate finite element discretization, the sway-rocking model produced satisfactory results with only the backfill characteristics as input. This illustrates the advantage of the CFM as flexible and easily applicable for fast assessment of the dynamic response of embedded structures.

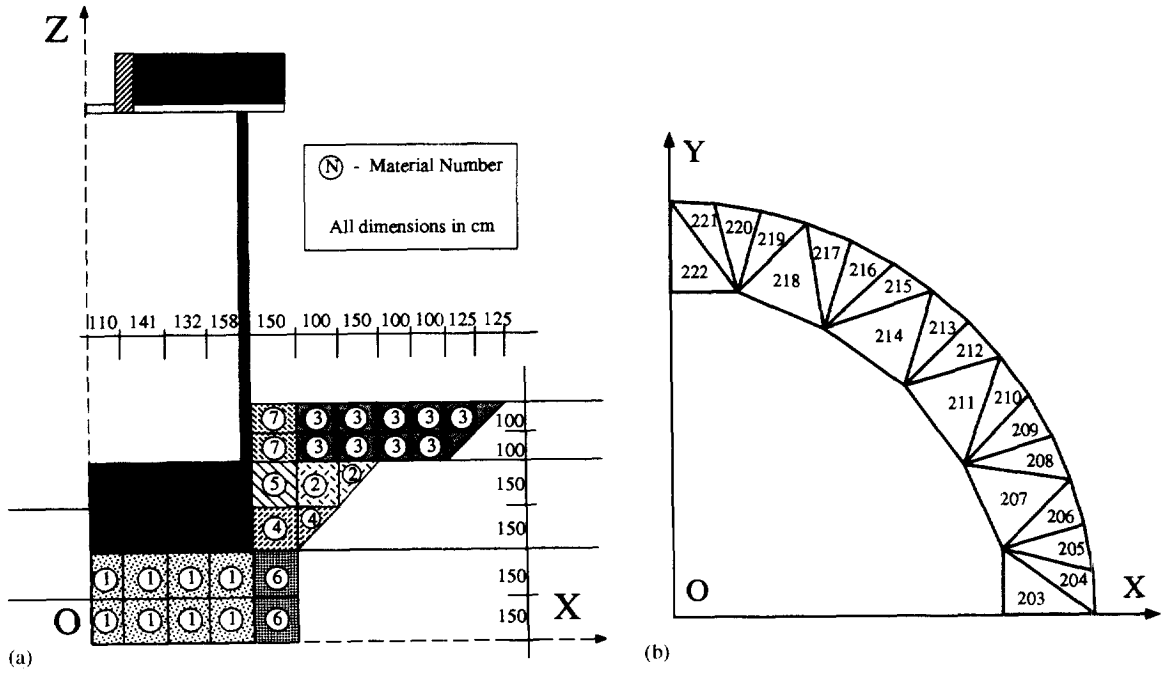

Fig. 10. FEM discretization of the soil–structure system (SASSI): (a) vertical cross-section of the model, (b) plan of the soft ring around the foundation.

Table 4. Soil properties used for dynamic analysis in D2 direction

Material type	Unit weight (g cm^{-3})	Poisson ratio	FVT Event 950530		Event 940120		Event 950501	
			Shear wave velocity (m s^{-1})	Damping ratio (%)	Shear wave velocity (m s^{-1})	Damping ratio (%)	Shear wave velocity (m s^{-1})	Damping ratio (%)
1	2.42	0.48	250	5	100	5	100	5
2	2.39	0.48	300	2	300	2	300	2
3	2.33	0.38	300	2	300	2	300	2
4	2.39	0.48	225	2	225	2	200	4
5	2.42	0.48	225	2	225	2	200	4
6	2.42	0.48	225	2	225	2	200	4
7	2.33	0.38	225	2	100	2	100	4

5.2 Microtremors

As was already shown, observation of ambient vibrations is an inexpensive and accurate alternative to forced vibration tests for identification of predominant system frequencies. However, serious problems with analysis of microtremors come from the difficulties in determination of the origin and nature of the excitation. In most cases, there is more than one source of vibration. These uncertainties obstruct conclusive quantitative evaluation of soil–structure system amplification.

It would be very practical to develop a methodology for accurate computation of system functions on the basis of microtremor data. In an attempt to provide a useful case study for this purpose, dynamic analysis of the soil–structure system was performed with SASSI. The microtremor record of the ground surface at an 8 m distance from the structure was input as control motion, employing a simplifying assumption that the excitation comes from a single source. The model validated by FVT-2 was used, but as explained earlier, the calculations had to be performed in the NS direction, so the properties of the layer below the foundation were averaged over those for the D1 and D2 directions.

When evaluating the free field response with SASSI, the user is given an opportunity to define the seismic environment [15]. The program first computes the site response to primary, shear and surface waves independently. Then the solution for each wave type is weighted by a frequency dependent factor called the 'participation ratio' and the results are superimposed to produce the combined response. The prescription of the individual values of the participation ratios is a matter of engineering judgment, but their total sum must be unity at each frequency. In most cases of earthquake response analysis, satisfactory results are achieved by assuming that only body waves propagate through the field. However, it is a well known fact that microtremors consist to a larger extent of surface waves, and for this reason in the present analysis shear and Rayleigh waves were considered. The fundamental mode of the Rayleigh wave was determined by the shortest wavelength method [5].

The amplitude of the simulated response was found to be dependent exclusively on the Rayleigh wave participation ratio, which was chosen constant over the whole frequency range. Its value was identified by trial and error in comparison of calculated and recorded microtremors at the top of the structure. Six records with length 20.48 s were extracted from the available record of length 150 s and each one was analyzed separately. They all yielded

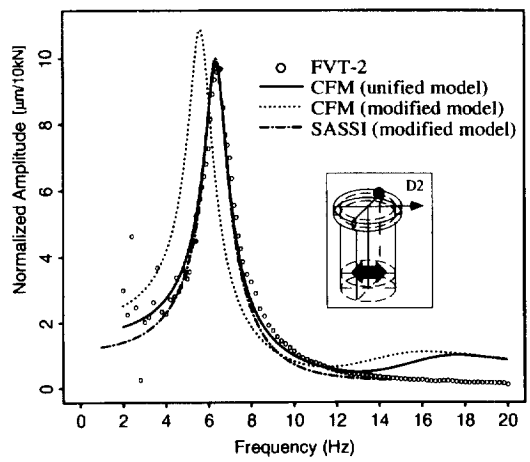

Fig. 11. Simulation of FVT-2 with CFM and SASSI.

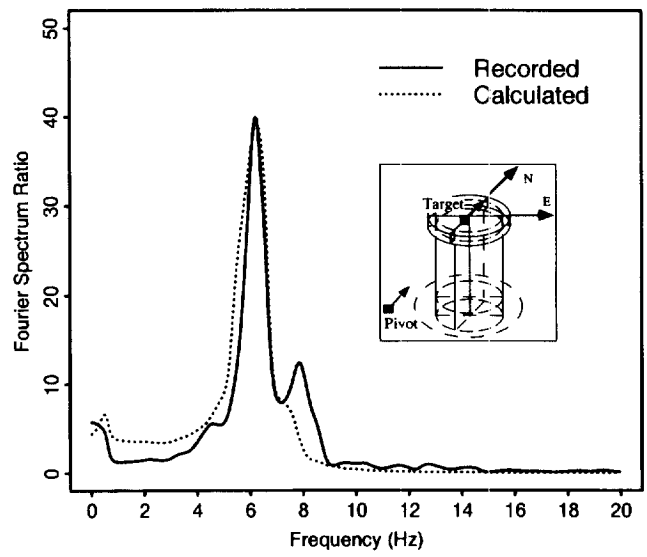

Fig. 12. Simulation of microtremor with SASSI.

substantially different best-fit values for the Rayleigh wave participation ratio. The ratio evaluated from the record with the highest coherence between free field and structural motion was accepted as the most reliable. Fig. 12 presents a comparison between recorded and calculated microtremor at the top of the structure in the NS direction. The Rayleigh wave participation ratio in this case is 39%.

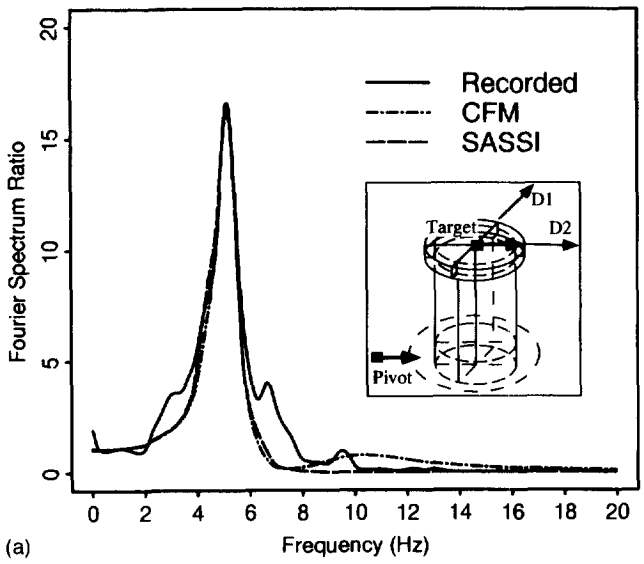

6 DYNAMIC RESPONSE TO LARGER EARTHQUAKES

In order to simulate properly the response of the soil–structure system during larger earthquakes, account had to be taken of the weakening of the soil support. In each case, the properties of the backfill zone were varied parametrically and identified by comparison of recorded and calculated structural response. Good agreement was achieved with both models for all the studied earthquakes. An example of the simulation of the D2 component of Event 950501 is presented in Fig. 13. In the frequency domain (Fig. 13(a)) the recorded and calculated Fourier spectrum ratios between the free field and the top of the structure are compared. In the time domain (Fig. 13(b)), the match of the recorded and computed time histories of acceleration response at the top of the structure is presented. The alterations of the parameters of each model are discussed in detail below.

6.1 Modification of the parameters of the sway-rocking model

The soil parameters of the sway-rocking model were adjusted to fit the recorded response by a trial and error procedure, developed by Ganev et al. [3]. Best-fit values of the soil stiffness and dashpot coefficients were determined for the two horizontal directions of each of the analyzed earthquake records. They are plotted against the peak ground velocity of the surrounding soil surface in Fig. 14.

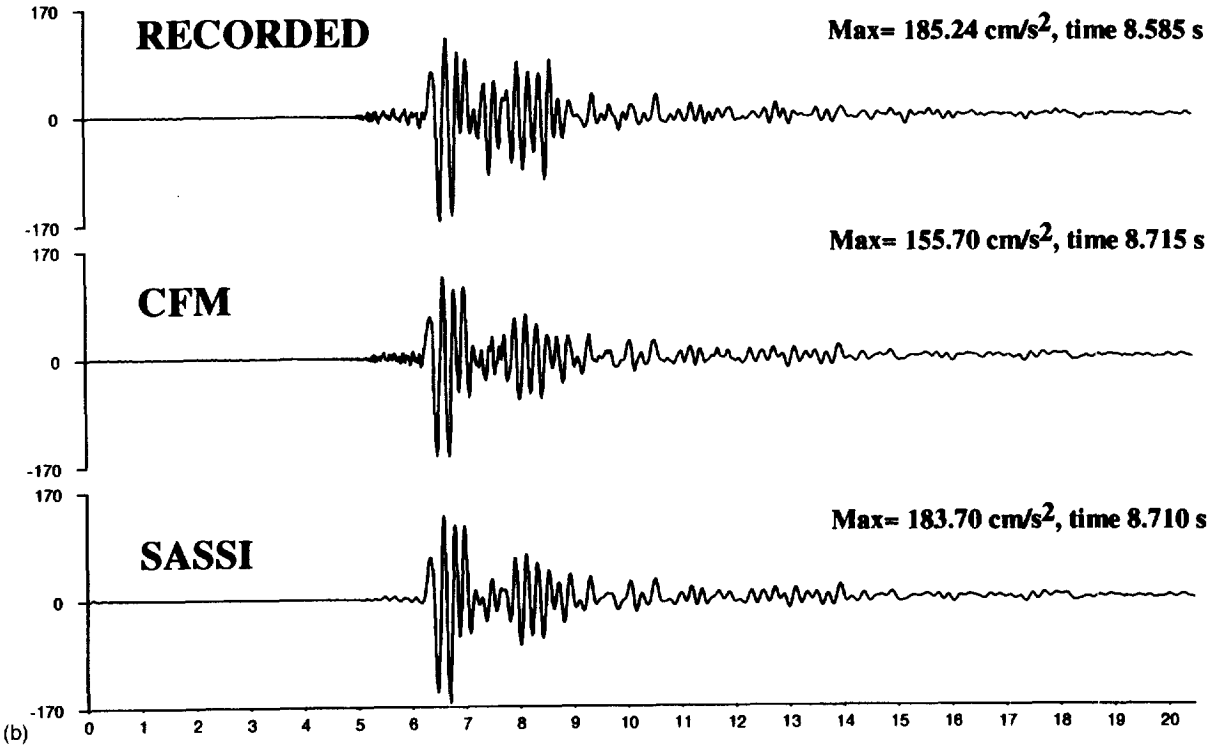

Fig. 13. Simulation of the D2 component of Event 950501 with CFM and SASSI: (a) Fourier spectrum ratios between the free field and the top of the structure, (b) recorded and calculated time histories of acceleration response at the roof top.

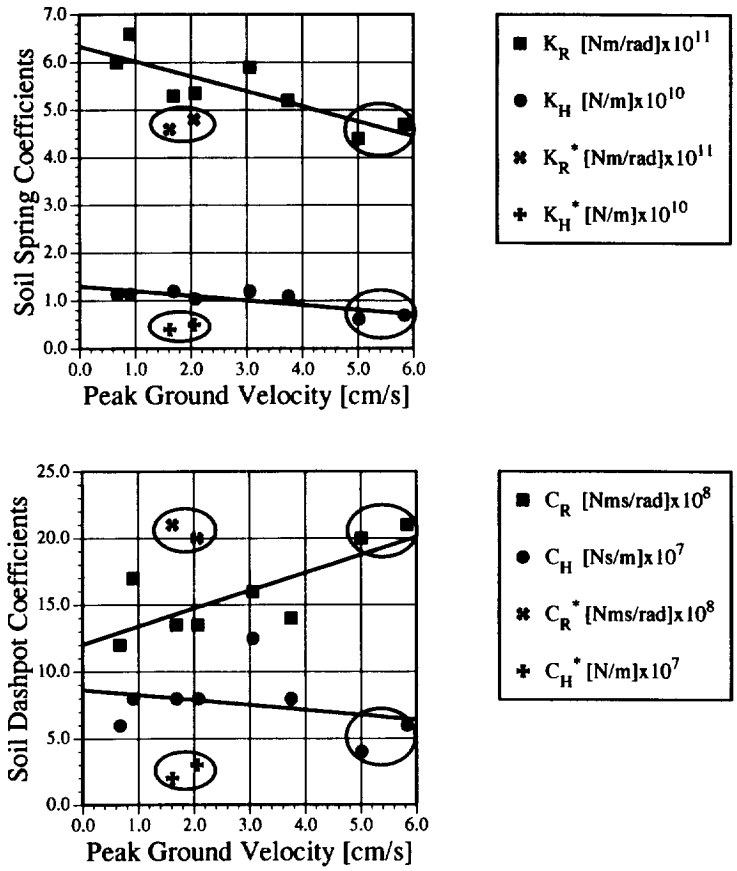

Fig. 14. Empirical relations between the peak ground velocity and the parameters of the sway-rocking model.

These empirical relations are similar to those derived by Ganev et al. [3] using data from a model structure built on a soft soil site in Chiba, Japan. A general decrease in the soil stiffness with increasing peak ground velocity is evident in both cases. It should be pointed out, however, that in the case of the Chiba tower, larger earthquake records were available and separation of structure from the soil was detected. Since no separation has been proven at the stiff soil site, it follows that the mechanism of soil stiffness degradation is different. As was previously mentioned, local non-linear effects are suspected to have caused this phenomenon.

The rocking damping coefficient at the soft soil site exhibited a decrease owing to separation, while in the Hualien case, a general increase is observed in accordance with the existing theory. However, no conclusive explanation can be offered at this time for the decrease in the sway dashpot constant at the stiff soil site.

The values denoted with a superscript (*) in Fig. 14 are from Event 950502. The size of this earthquake is commensurate with the moderate Events 940120 and 940605, but it occurred within a day after the larger Event 950501 (c.f. Table 2). For reference, the points corresponding to Event 950501 are also encircled in Fig. 14. It can be observed that the best-fit values for Event 950502 are closer to those of the preceding stronger earthquake rather than to those of the other similar events. Apparently the soil stiffness remained weakened for some time after the occurrence of Event 950501. As no newer data are available, the present status of the soil support cannot be evaluated. Considering, however, the values corresponding to Event 940120 and the following smaller Event 940530, it can be concluded that the effect is generally reversible with time. The same phenomenon was observed by Ganev et al. [3] at the soft soil site in Japan. In that case, the analyzed data showed that the degradation of the soil stiffness was, in general, reversed. It is interesting to point out that the rocking damping coefficient at the Hualien site preserved a higher value for the time period while the stiffness was lower.

6.2 Modification of the parameters of the finite element model

Monitoring the alteration of the springs of the sway-rocking model gives a general idea of the decrease in soil stiffness. At the same time, the analysis with SASSI enables a more precise assessment with regard to which particular backfill region undergoes changes during earthquakes. Compared to the model used for small strain level, the model which fits best the response of the moderate Event 940120 has softer elements of type 1 and type 7 (Fig. 10(a), Table 4). The best-fit model for the stronger earthquake Event 950501 is characterized with decreased stiffness of the whole annular

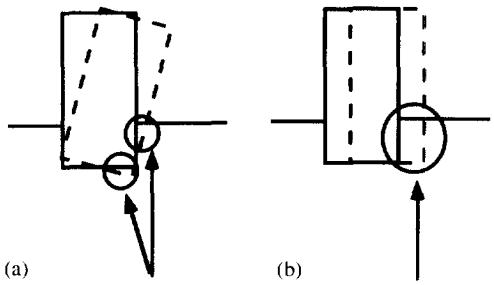

Fig. 15. Patterns of soil stiffness degradation in the near field zone: (a) regions degraded due to rocking, (b) regions degraded due to sway.

region of thickness 1.5 m (Fig. 10(a), Table 4). The physical meaning of these results can be illustrated with the help of Fig. 15. It shows the near field soil zones where the local stress concentration in contact with the foundation is likely to be the highest during rocking and sway. Rocking is the predominant mode of motion, corresponding to the fundamental frequency of vibration in all cases. During the moderate earthquake Event 940120 the sway mode ostensibly had a small contribution to the overall response and the near field soil degradation followed, by and large, the pattern shown in Fig. 15(a). During Event 940501, which had a larger horizontal ground acceleration, the sway mode had a more significant participation and the shape of the degraded zone was a combination of patterns shown in Fig. 15(a) and Fig. 15(b). For the purpose of numerical analysis it has been pragmatically assumed that the degradation extends uniformly as far as the soft annular region.

Under a dynamic load applied in the plane of symmetry *XOZ*, the largest shear strains ε_{zx} are experienced by the elements 203 to 207 (Fig. 10(b)), which extend from the ground level to a depth of 1.0 m below the surface. For each horizontal component of all the analyzed events the strains of these elements were evaluated and averaged. As this procedure utilized the already identified best-fit values of shear wave velocity (respectively shear modulus) and damping ratio of the surface layer, empirical relations of these parameters with the strains were easily constructed. For comparison, the non-linear elastic behavior of the same region was also evaluated analytically using the Ramberg–Osgood model. According to the formulation of this model, presented in Ref. [19], two parameters are required to constitute the skeleton curve of the stress–strain relationship: the reference strain γ_r and the maximum damping ratio h_{max}. The reference strain γ_r is by definition the shear strain at which the shear modulus reduces to 1/2 of its initial value. The maximum damping ratio h_{max} is the asymptotic value which the damping ratio approaches when the shear strain becomes infinitely large. Based on standard curves for gravel, γ_r was assumed equal to 0.0004 and h_{max} was assumed to be 0.25.

The empirical relation between the shear strain and the shear modulus reduction is compared with the theoretical curve in Fig. 16(a). There is a difference between the values identified with SASSI and with the Ramberg–Osgood model, particularly at strains larger than 4×10^{-4}. Disagreement can be seen also in the relation between the shear strain and the damping ratio in Fig. 16(b). It is obvious that the dynamic behavior of the soil support in this case cannot be described adequately with the non-linear elastic theory. Considering the absence of pore water pressure build-up or separation of soil from the structure, it is logical to blame the soil stiffness degradation on local non-linear effects, which are typically difficult to incorporate in a numerical model. Such rationalization is concurrent with the results of Tatsuoka et al. [20], who have shown experimentally that well graded gravel can be brittle under dynamic loading and local deformations can decrease its stiffness by up to 70%.

7 CONCLUSIONS

The dynamic behavior of a nuclear reactor containment model in Hualien, Taiwan was investigated using data from forced vibration tests (FVT), microtremor observations and earthquake records. A shift of the predominant frequency of the soil–structure system during earthquakes was observed. This phenomenon signifies degradation of the soil stiffness under large dynamic loads. A comparison with the results of Ganev et al. [3], from analysis of a rigid tower on a soft soil site in Japan, shows very similar phenomena. There is, however, some difference in the mechanism of

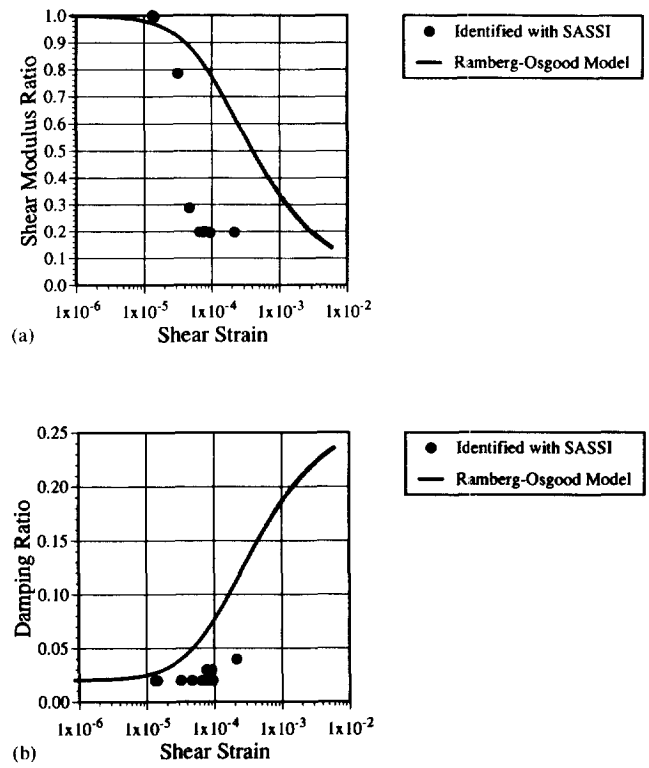

Fig. 16. Non-linear behavior of the backfill region: (a) shear modulus reduction vs. shear strain, (b) damping ratio vs. shear strain.

soil stiffness degradation. In the case of the soft soil site, separation of soil from the structure was detected and proven to be a more influential factor than non-linearity. The weakening of the soil stiffness, observed at the stiff soil site, is attributed to local non-linear effects.

The response of the containment model to FVT and earthquakes was simulated successfully with a sway-rocking model, whose soil parameters were evaluated on the basis of the continuum formulation method (CFM). Empirical relations between the peak ground velocity of different earthquakes and the soil stiffness and damping coefficients of this model were derived. It was used to demonstrate that the soil stiffness remained weakened for a certain time after a large earthquake and the rocking dashpot coefficient remained higher for the same period of time. Dynamic analysis was performed also with the finite element method, using the program SASSI with the flexible volume substructuring approach. This model produced a very good agreement with the recorded response and was used to investigate which zones of the backfill undergo changes during earthquakes. Using best-fit parameters of the supporting soil, identified in the analysis, empirical relations of the shear modulus reduction and damping ratio with the shear strain were constructed. Comparison with the theoretical curves evaluated on the basis of the Ramberg–Osgood model showed that the non-linear elastic theory could not describe adequately the dynamic soil behavior in this case.

It was demonstrated that microtremor observations can be a good alternative to forced vibration tests in the small strain range. An original numerical simulation of microtremors was performed. The participation ratio of Rayleigh waves in the ambient vibrations was determined by a parametric study.

Comparing the backfill properties used to achieve best-fit results with the two numerical models, it was concluded that the continuum formulation method tends to underestimate the soil stiffness. The reasons for this tendency are in the theoretical basis of the method and this should be expected upon application of other similar and popular methods of analysis as, for example, the Novak model. This conclusion has an important implication to design and might be of particular interest to practising engineers. Despite the shortcomings of the CFM, the satisfactory results achieved with this approach show that it has the advantage of being flexible and easily applicable for fast assessment of the dynamic response of embedded structures.

ACKNOWLEDGEMENTS

The authors would like to express their gratitude to Dr W. S. Tseng, President of International Civil Engineering Consultants, Inc., USA, Mr N. Nakamura of the Tokyo Electric Power Company (TEPCO), Japan and Dr S. Dermitzakis of Vectra Technologies Inc., USA for their indispensable help with the set-up and application of SASSI. The expert advice and suggestions of Professor T. Harada of Miyazaki University, Japan and Dr K. Yoshida of Izumi Research Institute, Shimizu Corporation, Japan are thankfully acknowledged.

REFERENCES

1. EPRI *Proceedings: EPRI/NRC/TPC Workshop on Seismic Soil–Structure Interaction Analysis Techniques Using Data from Lotung, Taiwan*, EPRI, Palo Alto, CA, 1987.
2. Tang, H.T., Stepp, J., Cheng, Y., Yeh, Y., Nishi, K., Iwatate, T., Kokusho, T., Morishita, H., Shirasaka Y., Gantenbein F., Touret, J., Sollogoub, P., Graves, H. & Costello, J. The Hualien large-scale seismic test for soil–structure interaction research. *Transactions of the Eleventh International Conference on Structural Mechanics in Reactor Technology*, Tokyo, Japan, 1991, K04/4, pp. 69–74.
3. Ganev, T., Yamazaki, F. & Katayama, T. Observation and numerical analysis of soil–structure interaction of a reinforced concrete tower. *Earthquake Engineering and Structural Dynamics*, 1995, **24**, 491–503.
4. Kokusho, T., Nishi, K., Okamoto, T., Kataoka, T., Tanaka, Y., Kudo, K., Tang, H.T. & Cheng, Y. H. Geotechnical investigation in the Hualien large scale seismic test project. *Transactions of the Twelfth International Conference on Structural Mechanics in Reactor Technology*, Stuttgart, Germany, 1993, K03/4, pp. 85–90.
5. Kokusho, T., Kudo, K., Okamoto, T., Tanaka, Y., Kawai, T., Sawada, Y., Yajima H. & Suzuki, K. Soil–structure interaction research of a large-scale model structure at Hualien, Taiwan (Part 1). *Proceedings of the Ninth Japan Earthquake Engineering Symposium*, Vol. 2, Tokyo, Japan, 1994, pp. 1369–1374.
6. Ganev, T., Yamazaki, F., Katayama T. & Ueshima, T. Soil–structure interaction of a containment model in Hualien, Taiwan. *Proceedings of the Twenty-third JSCE Earthquake Engineering Symposium*, Tokyo, Japan, 1995, pp. 397–400.
7. Yamazaki, F., Lu, L. & Katayama, T. Orientation error estimation of buried seismographs in array observation. *Earthquake Engineering and Structural Dynamics*, 1992, **21**, 679–694.
8. Morisita, H., Tanaka, H., Nakamura, N., Kobayashi, T., Kan S., Yamaya H. & Tang, H.T. Forced vibration test of the Hualien large scale SSI model. *Transactions of the Twelfth International Conference on Structural Mechanics in Reactor Technology*, Stuttgart, Germany, 1993, K02/1, pp. 37–42.
9. Tanaka, H., Sugiyama, T., Kobayashi T. & Yamaya H. Forced vibration test of the Hualien large scale SSI model (Part 2). *Proceedings of the Ninth Japan Earthquake Engineering Symposium*, Vol. 2, Tokyo, Japan, 1994, pp. 1387–1392 (in Japanese).
10. De Barros, F.C.P. & Luco, J.E. Identification of foundation impedance functions and soil properties from vibration tests of the Hualien containment model. *Soil Dynamics and Earthquake Engineering*, 1995, **14**, 229–248.
11. Harada, T., Kubo, K. & Katayama, T. Dynamic soil–structure interaction analysis by continuum formulation method. *Report of the Institute of Industrial Science*, Vol. 29, University of Tokyo, Japan, 1981, pp. 139–194.
12. Harada, T. & Kubo, K. Evaluation of dynamic stiffness of embedded foundation using dynamic reaction of surface layer. *Proceedings of the Seventh World Conference on Earthquake Engineering*, Vol. 5, Istanbul, Turkey, 1980, pp. 197–204.
13. Harada, T., Kubo, K. & Katayama, T. Dynamic soil reactions (impedance functions) including the effect of dynamic response of surface stratum. *SeisanKenkyu, Monthly Journal*

of the Institute of Industrial Science, University of Tokyo, Japan, 1979, **31**, (9–11).
14. Harada, T. & Kubo, K. Dynamic (complex) stiffness and vibration of embedded cylindrical rigid foundation. *Proceedings of the Fifth Japan Earthquake Engineering Symposium*, Tokyo, Japan, 1978, pp. 401–408.
15. Lysmer, J., Ostadan, F., Tabatabaie, M., Vahdani, S. & Tajirian, F. *SASSI, A System for Analysis of Soil–Structure Interaction, User's Manual*. University of California, Berkeley, CA, 1988.
16. Veletsos, A. & Dotson, K. Horizontal impedances for radially inhomogeneous viscoelastic soil layers. *Earthquake Engineering and Structural Dynamics*, 1988, **16**, 947–966.
17. Tang, H.T. & Nakamura, N. Analysis of the forced vibration test of the Hualien large scale soil–structure interaction model using a flexible volume substructuring method. *Proceedings of the Third JSME/ASME Joint International Conference on Nuclear Engineering, (ICONE-3)*, Vol. 4, Kyoto, Japan, 1995, pp. 2053–2058.
18. Beredugo, Y.O. & Novak, M. Coupled horizontal and rocking vibrations of embedded footings. *Canadian Geotechnical Journal*, 1972, **9**, 477–497.
19. Katayama, T., Yamazaki, F., Nagata, S., Lu, L. & Turker, T. A strong motion database for the Chiba seismometer array and its engineering analysis. *Earthquake Engineering and Structural Dynamics*, 1990, **19**, 1089–1106.
20. Tatsuoka, F., Teachavorasinskun, S., Dong, J., Kohata, Y. & Sato, T. Importance of measuring local strains in cyclic triaxial tests on granular materials. *Proceedings of the American Society of Testing and Materials*, Vol. 2, ASTM STP 1213, Philadelphia, PA, 1995, pp. 322–336.